THE PHOTOGRAMMETRIC RECORD

The Photogrammetric Record 27(137): 111–126 (March 2012)
DOI: 10.1111/j.1477-9730.2011.00672.x

CLOSE RANGE STEREOPHOTOGRAMMETRY AND VIDEO IMAGERY ANALYSES IN SOIL ECOHYDROLOGY MODELLING

María J. Rossi (rossi@cenpat.edu.ar)
Jorge O. Ares (joares@cenpat.edu.ar)
National Patagonic Centre/CONICET, Puerto Madryn, Argentina

Abstract

Ecohydrology is an emerging discipline in the environmental sciences. Soil micro-relief is of relevance to various ecohydrological processes such as rainwater redistribution, seed displacement through water runoff, water erosion and plant competition for water. Mechanical–optical methods to characterise the soil surface and its incidence in these processes are time consuming and can produce modifications of soil relief. This research explores a methodology combining non-contact techniques (close range stereophotogrammetry and geostatistical modelling) for microtopographic description with video imagery analysis to formulate quantitative determination of surface water movement and infiltration in undisturbed field plots. The numerical quality of the results obtained was tested with ad hoc laboratory models representing various elementary landforms (basin, hill and ridge), as well as with infiltration runoff experiments in undisturbed field plots. The requirements to define a minimum set of properly oriented digital images to attain target precision thresholds in modelling soil microtopography for ecohydrological applications are shown as well as the conditions and experimental arrangement to obtain adequate video imagery of water movement on the soil surface. The use of geostatistical algorithms to analyse ecohydrological processes occurring at the soil surface is illustrated with results obtained from field plots. The methodology presented serves to characterise and quantify water-related ecological processes occurring at the soil surface while preserving undisturbed soil conditions. Potential applications are in ecohydrology, soil erosion science and environmental material transport studies.

Keywords: close range stereophotogrammetry, digital elevation models, ecohydrology, soil water, soil water runoff

Introduction

This study is in line with previous work of the research team in Terrestrial Ecology at the National Patagonic Centre in Chubut, Argentina, on the sustainability of vegetation of the Patagonian Monte; this is a landscape form occupying 250 000 km^2 in the central region of the country and the northern Patagonian region. Similar landscapes are extensively found in

arid and semi-arid climates worldwide (Mares et al., 1985). The mean annual precipitation in such areas is usually below 20 cm, and the vegetation canopy is distributed as patches of various shrubs with perennial grasses sparsely distributed among areas of bare soil. Golluscio et al. (1998) reported that large quantities of summer precipitation were used differently by shrubs and perennial grasses. Ares et al. (2003) showed that the early stages of desertification were characterised by a progressive uncoupling of the spatial patterns of plant arrangements and water runoff, indicating that changes in the water balance at various vegetation patches altered the interactions among the component plant forms, thus altering their ecological performance. These findings were partially included in the construction of a spatial cell-explicit model (resolution of 150 mm × 150 mm) of the dynamics of shrub and perennial grass patches, which was tested in areas with various degrees of desertification (Bisigato et al., 2002).

Rainwater redistribution on the surface of the soil is a particularly relevant process in modelling the distribution and conservation of vegetation in semi-arid and arid regimes (Schlesinger et al., 1999; Tongway and Ludwig, 1999). Recent theories state that plant spatial arrangements, as encountered in such areas worldwide, are bound to low-productivity environments and result from a self-organising process involving water distribution (Deblauwe et al., 2008). The present research aims to supply improved quantitative tools to estimate ecohydrological parameters related to surface water redistribution among plant forms in the study area. The techniques and results would be relevant for relatively flat semi-arid and arid areas worldwide (Zhao et al., 2011).

Ecohydrology has been identified as an emergent paradigm in the environmental sciences, aiming to understand and develop quantitative models of the interactions among the physical aspects of the environment, water and organisms at various spatial scales (Zalewski and Robarts, 2003; Hannah et al., 2004). Ecohydrology processes at the soil surface involve factors determining rainwater runoff and redistribution over the soil surface (Planchon et al., 2002; Liu and Singh, 2004), water infiltration into the soil profile (Wallach et al., 2001; Li et al., 2005), plant competition for water uptake (Puigdefábregas et al., 1996; Solé-Benet et al., 1997), soil–water erosion (Liu and Singh, 2004; Rieke-Zapp and Nearing, 2005), the movement of seeds and wind transported materials (Cerdá and Garcia-Fayos, 1997), and the distribution of soil nutrients in the upper soil profile (Frere et al., 1980; Gburek and Sharpley, 1998).

Water movement at the soil surface is a highly dynamic process occurring over short time periods. Conceptual models of the processes involved usually include considerations of soil microtopography and roughness (Jester and Klik, 2005; Aguilar et al., 2009), soil slope gradients (Solé-Benet et al., 1997; Puigdefábregas et al., 1998) and upper soil permeability (Ritsema and Dekker, 1995; Li et al., 2005). The pattern of surface soil microtopography (usually in height ranges of a few millimetres) modifies the redistribution of water during rain events (Helming et al., 1993; Kamphorst and Duval, 2001).

Various authors developed techniques to characterise soil microtopography, including mechanical (Planchon et al., 2002; Jester and Klik, 2005), laser altimetry (Huang et al., 1988; Kamphorst and Duval, 2001; Martin et al., 2008) and close range photogrammetric methods (Warner, 1995; Merel and Farres, 1998; Stojic et al., 1998; Rieke-Zapp et al., 2001; Aguilar et al., 2009). The most promising methods for micro-relief data acquisition are non-contact methodologies that do not alter the soil surface. Merel and Farres (1998) used stereophotogrammetry to quantify changes in soil micro-relief in plots under 1 m^2. Arias et al. (2007) used stereophotogrammetry to generate landscape-scale digital elevation models (DEMs). Rieke-Zapp et al. (2001) and Brasington and Smart (2003) applied photogrammetric methods and obtained results of the order of centimetres; Warner (1995) and Rieke-Zapp and Nearing (2005) claim millimetre order results. Aguilar et al. (2009) used close range stereophotogrammetry (CRS) and focused on the general problem of characterising soil microtopography,

achieving precisions in the range of millimetres in altitude estimates with small field plots. They also raised concerns about the eventual consequences of errors in the estimation of smoothed surfaces of DEMs for the analysis of some complex hydrological characteristics like the connectivity of runoff flows.

After the coordinates of the sample points have been estimated through CRS, an estimation of the coordinates of numerous other points of the photographed surface is needed in order to construct a DEM. The estimation is accomplished through geostatistical modelling procedures involving the use of an algorithm describing the variability of altitude across the surface. The algorithm uses the semi-variogram, a function of distance among points describing the correlation of altitudes observed between sample locations. The semi-variogram is commonly represented as a scatter graph with points representing the variance of altitude (graph ordinate y) at increasing distances (graph abscissa x) between all pairs of sampled locations. Such a graph is called an experimental semi-variogram because the point values correspond to those of experimental samples. A curve (usually a power function) fitted to these points constitutes a theoretical semi-variogram that is used to estimate the altitude values corresponding to non-sampled points, thus generating a smoothed surface estimate (kriging) (Isaaks and Srivastava, 1989; Goovaerts, 1997).

The objective of this research is to explore a methodology combining non-contact techniques (close range stereophotogrammetry and geostatistical modelling) for microtopographic description and video imagery analysis to formulate quantitative analyses of the processes involved in surface water movement and infiltration in undisturbed field plots. The spatial scale of the observations has been chosen to be compatible with the previous work of the research team on distributed modelling of the dynamics of the vegetation canopy in the semi-arid Patagonian Monte region of Argentina (Bisigato et al., 2002; Ares et al., 2003). The techniques were tested on laboratory landform models and applied to undisturbed soil plots in a semi-arid area.

Materials and Methods

The following two hypotheses were formulated and tested in this research:

(1) *Hypothesis 1* (H1). Close range stereophotogrammetry (CRS) can supply sufficient information on soil microtopography for ecohydrological purposes to allow geostatistical modelling (GSM) of the undisturbed surface of soil plots at a reasonable ratio of effort to accuracy and precision.
(2) *Hypothesis 2* (H2). Surface soil water movements can be monitored and quantified through rectified video image (RVI) analysis based on models developed through CRS-GSM.

Hypothesis 1: CRS-GSM

Calibration through Laboratory Landform Models; Application to Soil Plot Scale. Laboratory landform models were built representing areas of three basic landforms (basin, hill and ridge) with target points representing terrain altitudes marked at the centre of small cuboidal wooden blocks of varying heights in the range 1 to 15 mm, mounted on a rigid wooden base (reference x–y plane). Nine vertical, plastic-headed spikes of known height (50 mm) were used to generate 18 control points. These were the top and base of the following: four spikes at the mid-points of the plane sides; four at the corners of a virtual internal square

with sides parallel to those of the model plot and about half of its total surface; and one at the centre of the model, whose top was defined as the x–y–z coordinate origin (Fig. 1). The x–y coordinates of all the points were measured with an accuracy of 0·5 mm, and the z coordinate to 0·1 mm, by means of a micrometer calliper.

Images of the models (3072 × 2304 pixels) were obtained with a digital camera (Kodak EasyShare Z712 IS 7·1 MP; focal length of 5·32 mm), set to ''manual'' mode and ''normal'' focus. The camera's optical parameters were recalibrated with the specific self-calibration module of the i-Witness application (DeChant Consulting Services, Bellevue) and the bundle adjustment was solved with the same package, performing numerous exploratory tests to optimise the geometry of the image network. To this end, a rejection threshold of the overall RMSE of greater than 1·5 mm in the image referencing coordinates was adopted.

Following exploratory tests, a procedure was adopted using three replicates of five images taken at normal and oblique positions (see Fig. 2) with respect to the reference plane of each landform model. All images covered the whole test area and all the control points. All target points simulating terrain level at the top of the wooden blocks were identified in all five photographs by using an automatic centring tool built in the i-Witness application. Manual corrections of the estimated point positions were made to an accuracy of less than 1 pixel (0·32 mm × 0·43 mm) of positional difference among the images. A segment of known length along the x coordinate axis was identified in order to set the scale and length units. In order to define a coordinate system centred on the model plot, the measured coordinates of the control points were introduced by importing them in a text file into the CRS application, which linked the coordinate system defined by control points with the remainder of the points identified on the plot images. In certain cases, additional manual corrections to some of the point coordinates

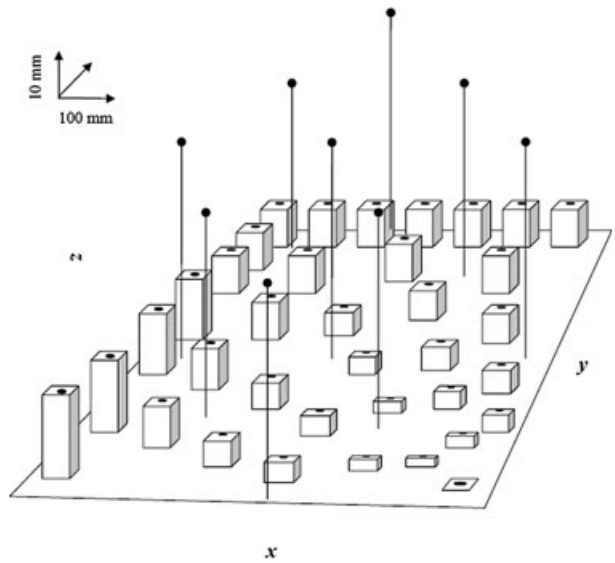

FIG. 1. Schematic view of a laboratory landform model (basin) used to test the accuracy and precision of the CRS routine used in this study. Tops and bases of plastic-headed spikes provided 18 control points. Simulated terrain points are marked on the top of the wooden cuboids. Scale along the z axis is stretched to enhance visibility. Similar models (not shown) were built to represent the ridge and hill landforms.

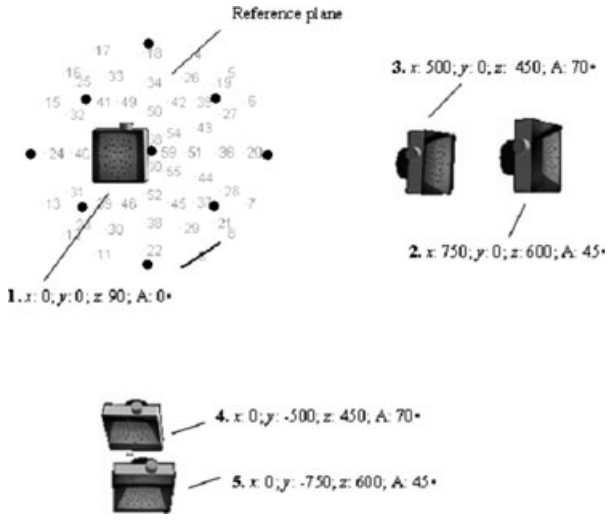

FIG. 2. Configuration of the image net used for CRS of both experimental and field plots in this study, combining normal position (1) and oblique camera locations (2 to 5) with respect to the reference plane of a landform model. Model coordinates (mm) of each camera location with respect to the origin at the centre of the reference plane are given. View angles A are with respect to the vertical. Light grey numbers indicate the location of target points. Dark dots indicate the location of the nine control spikes. The calibration length segment is the line at the bottom right.

were necessary as identified by inspecting the residuals between a priori and a posteriori bundle calculations performed by the application.

The accuracy of the CRS process performed on laboratory models was tested through the slope parameter of Type I linear regression models (Weisberg, 2005) (slope = 1·00 meaning full accuracy) of the measured versus the CRS-estimated x, y, z coordinate values of the target points, while the precision of the process was evaluated through the normalised (percentage of mean coordinates) rms values of the deviates of the estimated values with respect to the regression fit.

In the case of the field plots, a regression fit was calculated through the error-in-variable model (EVM; regression Type II in Reilly et al. (1993)) where direct estimates of coordinates of selected target points were obtained either through tape measurements alone or through these combined with optical level readings of the z coordinate.

The average of the three sets of coordinates of each estimated landform model was used to calculate a DEM of each landform by exporting the coordinates of the estimated point grid to the Surfer application (v. 7.0; Golden Software, Colorado) through text files. Furthermore, the theoretical semi-variograms (Goovaerts, 1997) were estimated through the expression

$$v = am^b \tag{1}$$

where v is a theoretical omnidirectional semi-variogram, m is the lag or interval calculation, and a and b are scale and power parameters fitted to the experimental data. Based on the theoretical semi-variograms, the coordinates of non-sampled points at various grid densities were estimated using a kriging algorithm (Goovaerts, 1997; Houlding, 2000) to obtain DEMs of the laboratory landforms. The same method was applied to obtain the DEMs of five undisturbed field plots of about 0·7 m^2. To this end, 64 points were represented on the soil surface by means of plastic red beads (3 mm diameter) distributed at the corners of a virtual,

regular grid encompassing the whole terrain under analysis. Ten centimetre needles inserted vertically (as checked with a level bubble) into the ground were used to create control points and all needle tops were levelled to the same height (above a reference plane) by means of a 700 mm long carpenter level. A set of images as indicated in Fig. 2 was obtained and a CRS and statistical model analysis of the coordinate estimates of control points was tested as in the case of the laboratory models in order to estimate the accuracy and precision of coordinate estimates.

Additionally, a vector map was created through the Surfer application representing the field of surface runoff vectors of the field plots as inferred from the DEM. The two components of the vector map, direction and magnitude, were automatically generated from a single grid by computing the altitude gradients among pixels of the represented surface. At any given grid node, the direction of the arrow indicates the steepest gradient, and the length of the arrow indicates the magnitude of the gradient.

In order to obtain independent estimates of the accuracy and precision of the CRS applied to field plots, a DEM of a field plot was also obtained through a direct optical method. A Kern GK1-AC optical level was placed at about 5 m in the x direction from the centre of the plot coordinate origin, and readings from a survey staff with millimetre graduations, alternately placed on the bead and control point locations, were obtained. The x, y, z coordinate estimates were then processed through GSM as previously described.

Hypothesis 2: CRS-GSM-RVI

Field Validation with Irrigation Experiments on Field Plots. After performing a CRS-GSM analysis of the field plots, a lightweight (2 kg), portable, wind-protected nozzle irrigation system was mounted on a wooden frame and adjusted with a pressure gauge and calibrated nozzle to variable irrigation rates (70 to 270 cm^3/min), known to be enough to exceed the water infiltration rate in soil, over variable time intervals in the range of 2 to 20 min. The irrigator frame also supplied support for a camera (Kodak EasyShare Z712 IS 7·1 MP; video mode) located at a near-zenith position over the centre of the plot and about 1 m above ground level. An irrigation event was then started and continued until the water runoff plume reached some of the borders of the video image in any direction.

Images of videos obtained during the irrigation event were retrieved every 0·1 min, exported to an image processing application (Idrisi v. 14.02, ClarkLabs, Worcester) and resampled to obtain orthorectified views. The DEM of the plot created through the analysis with the Surfer application was imported in the form of a digital layer, together with the corresponding map of water flow vectors, and overlaid on the re-projected video images. The advances of the runoff plume were then inspected and compared with the estimated flow directions at successive time intervals (0·1 min), and the plume area and altitude gradients in the direction of water flows around the plume were measured.

RESULTS

Hypothesis 1: CRS-GSM

Table I shows the results of the camera calibration and settings used during the CRS analyses. Corrections to the camera parameters corresponding to each set of images from the same bundle adjustment were introduced by the automatic adjustment tool built into the i-Witness application.

TABLE I. Camera type and example of calibration parameters.

Camera parameters	*Values*
Model	Kodak Z712 IS
Resolution (pixels)	3072 × 2304
Pixel size (mm)	0·0016 × 0·0016
Focal length (mm)	5·3228

The CRS-GSM procedure demanded about 30 min for the installation of control points and picture taking, 60 min for CRS projection and 15 min for the GSM. Table II shows the variability among replicated CRS procedures performed on the same laboratory model, as estimated through the RMSE. Fig. 3 shows the experimental and fitted theoretical variograms corresponding to the laboratory landform DEMs. Table III shows the linear regression fits and corresponding RMSE of deviates on all three coordinate estimates. Fig. 4(a) shows an example

TABLE II. Precision estimates of replicates of CRS on three laboratory landform models.

	Basin			*Hill*			*Ridge*		
Replicate	1	2	3	1	2	3	1	2	3
RMSE (mm)	0·5	0·3	0·3	0·4	0·3	0·2	0·3	0·3	0·2

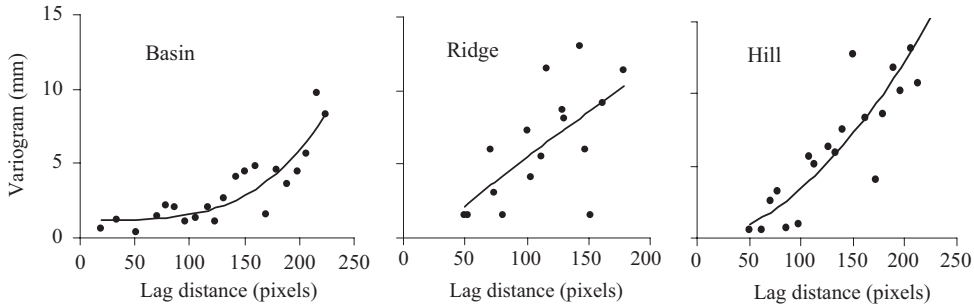

FIG. 3. Experimental (dots) and theoretical (power fitting line) variograms corresponding to the three laboratory landform models under study.

TABLE III. Results of the CRS applied to laboratory landform models and field plots. Regression fit ($p < 0{\cdot}001$) and normalised RMSE of measured (m) versus estimated (e) coordinates of all models. All units are millimetres.

	z	x	y
		Basin	
Fit	$z_m = 1{\cdot}03(\pm 0{\cdot}022)z_e$	$x_m = 1{\cdot}003(\pm 0{\cdot}005)x_e$	$y_m = 1{\cdot}001(\pm 0{\cdot}005)y_e$
RMSE	4·24	0·66	0·66
		Hill	
Fit	$z_m = 0{\cdot}979(\pm 0{\cdot}025)z_e$	$x_m = 0{\cdot}993(\pm 0{\cdot}002)x_e$	$y_m = 1{\cdot}001(\pm 0{\cdot}002)y_e$
RMSE	6·22	0·33	0·38
		Ridge	
Fit	$z_m = 0{\cdot}981(\pm 0{\cdot}035)z_e$	$x_m = 1{\cdot}001(\pm 0{\cdot}002)x_e$	$y_m = 1{\cdot}001(\pm 0{\cdot}002)y_e$
RMSE	3·89	0·65	0·69
		Field plots	
Fit	$z_m = 1{\cdot}002(\pm 0{\cdot}001)z_e$	$x_m = 1{\cdot}00(\pm 0{\cdot}002)x_e$	$y_m = 0{\cdot}998(\pm 0{\cdot}003)y_e$
RMSE	6·46	1·34	1·69

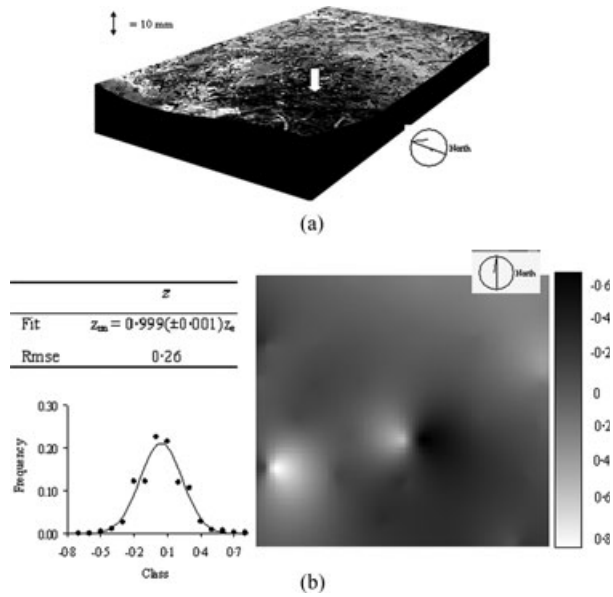

FIG. 4. (a) 3D view DEM of field plot 1 estimated with CRS-GSM with draped RVI image obtained 180 s after the start of irrigation. The arrow indicates the centroid of the irrigated area. Note the runoff plume advance towards the central micro-depression in the plot. (b) Right: spatial distribution of errors in z estimates on the DEM of the same plot with respect to the estimated true value obtained with EVM based on a similar DEM produced with an optical level method. Left: EVM fit and frequency distribution of EVM-based values.

of a 3D view of a field plot where both CRS-GSM and optical-level-based DEMs were constructed. The advance of a runoff plume observed after 180 s from the start of irrigation is shown in the direction of a central depression in the plot. Fig. 4(b) shows a map of (normally distributed) errors of the z coordinate as estimated through the EVM algorithm.

Hypothesis 2: CRS-GSM-RVI

Water Runoff Plume and Water Flow Analyses in Field Plots. In addition to the processing times described in the previous section, the RVI analyses performed on field plots required about 180 min per plot. Fig. 5 shows the correspondence of water flow vector fields (as estimated from DEMs of field plots) with the direction of movement of the water runoff plumes during the irrigation experiments. Fig. 6 shows the analyses of two irrigation experiments with similar flow, on field plots with soils of similar textural composition and differing slopes. Several dynamic, interrelated parameters useful in describing water-related dynamic processes (infiltration, runoff, ponding) at the plots were estimated:

$$\mathrm{W/I} = f(\mathrm{I_r}, \mathrm{P_r}) \tag{2}$$

$$\mathrm{RPL} = f(\mathrm{SRA}, \mathrm{I_{rr}}, \mathrm{I_r}, \mathrm{P_r}) \tag{3}$$

$$\mathrm{ROS} = f(\mathrm{SRA}, \mathrm{I_{rr}}, \mathrm{I_r}, \mathrm{P_r}) \tag{4}$$

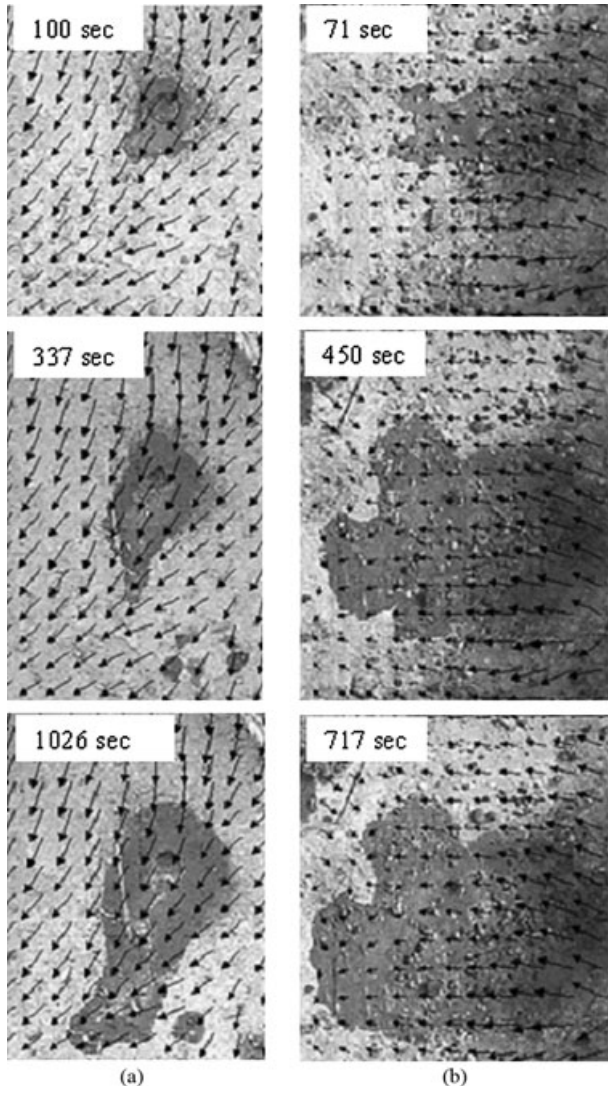

FIG. 5. Analyses of rectified video imagery (RVI) of field plots 2 (left sequence (a)) and 3 (right sequence (b)) at successive time intervals after the initiation of irrigation experiments. Rectified images of water flow vector field are overlaid on terrain RVIs at an *x*–*y* resolution of 50 mm × 50 mm. Circles indicate the irrigated area.

where W/I is wet area/irrigated volume, RPL is runoff wetted area (plume) longest length, ROS is the runoff speed, I_{rr} is the irrigation rate, I_r is the infiltration rate, P_r is the ponding rate and SRA is slope along runoff axes.

Plot A

Parameter	Definition	Value	Units
W/I	Wet area/Irrigated volume	2·27 ±0·08	cm^2/cm^3
SRA	Slope along runoff axes	0·21	cm/cm
		0·18	cm/cm
RPL	Runoff plume length	40·4	cm
		38.5	cm
ROS	Runoff speed (Δ wet area/time)	9·93 ±1·3	cm^2/sec

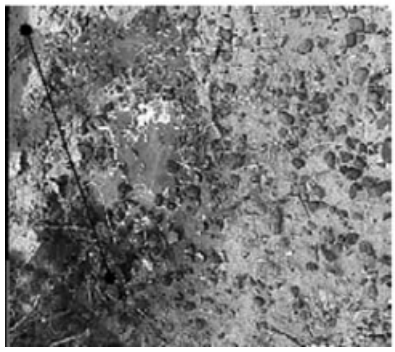

Plot B

Parameter	Definition	Value	Units
W/I	Wet area/Irrigated volume	1·52 ±0·05	cm^2/cm^3
SRA	Slope along runoff axes	0·09	cm/cm
RPL	Runoff plume length	43·3	cm
ROS	Runoff speed (Δ wet area/time)	1·38 ±0·3	cm^2/sec

Fig. 6. Quantitative results of the CRS-GSM-RVI technique applied to the analysis of irrigation experiments at two field plots where different degrees of runoff, infiltration and ponding occurred. Top: low ponding, fast development of runoff plumes. Bottom: high ponding, slow runoff plume development.

Discussion

Hypothesis 1. Close range stereophotogrammetry (CRS) can supply sufficient information on soil microtopography for ecohydrological purposes to allow geostatistical modelling (GSM) of the undisturbed surface of soil plots at a reasonable ratio of effort to accuracy and precision.

In this study, simple laboratory landform models (basin, hill and ridge) of about 1 m^2 and maximum heights of under 12 mm, together with field plots at similar scales, were used to obtain calibrations of a CRS procedure with a set of normal and oblique convergent images obtained with a standard camera (Table I). The procedure yielded estimates of x, y, z coordinates of the laboratory models accurate to less than 3·5%. Precisions were under 1·5% of the mean range of coordinate variation in the x, y coordinates and less than 7% in the z coordinate, which means sub-millimetre results in the latter (Table III). Lower accuracy and precision (but still in the millimetre range) were attained by CRS estimates of the field plots; this is a probable consequence of the inherent difficulties in obtaining high quality coordinate measurements under field conditions.

The convenience of adopting an image net with oblique camera configurations was highlighted in a similar study with larger plots (1·4 m × 3·9 m) by Heng et al. (2010) who were

interested in characterising soil microtopography for soil erosion studies with various geometric configurations of tie and control points. Additionally, this study indicates that a CRS configuration involving combinations of normal and oblique convergent images proved efficient in attaining adequate accurate and precise coordinate estimates in a reasonable timeframe. Recently reported research shows that using mildly non-vertical convergent imagery for DEM generation minimises the remaining systematic error surfaces or domes caused by slightly inaccurately estimated lens distortion parameters (Wackrow and Chandler, 2011).

The selection of the statistical procedures to evaluate the quality of a CRS also deserves further analysis. While the RMSE (and its precision equivalent) is a widely used parameter to quantify a CRS procedure, it is a global estimate of the accuracy of the CRS and does not give information on how the errors are distributed at various ranges of the estimate values, nor does it distinguish between systematic under/over-estimation. In this study, regular regression analysis (Type I regression) was used to estimate the accuracy of CRS estimates from coordinate values in small laboratory models. Regression Type I of two variables (in this research tape-measured coordinate values, here called ''direct measurements'', versus CRS or ''estimates'') assumes that a comparison is performed between a variable measured *almost* without error (independent) and another one (dependent) measured with an unknown error. This assumption seems reasonable in the case of laboratory models of small dimensions, where coordinates of the target points model can be directly measured with high accuracy through 0·5 mm scaled rules, callipers, etc. This criterion is adopted in this study.

In the case of field plots, accurate direct coordinate measures needed to calibrate CRS are difficult to obtain because of abrupt terrain changes, pebbles, plants, meteorological conditions and related factors. In other cases, a comparison is desirable between two non-direct techniques such as CRS and an optical level or laser scanner. In these cases, both sets of coordinate estimates can be anticipated to be affected by errors, and a Type I regression can no longer be assumed as an appropriate statistical model to relate them (Fekri and Ruiz-Gazen, 2006). Alternatively, an EVM procedure (regression Type II) is appropriate, where both the CRS and the direct measurements are considered as dependent. The EVM algorithm used in this study was supplied by Reilly et al. (1993) and essentially consists of a convergent procedure to estimate so-called true coordinate values based on measurements obtained with unknown errors using both CRS and direct measurements or optical level techniques. RMSE values can then be computed from the deviations of a regression Type I model relating each dependent variable to the true estimate of both.

Based on the results presented above, it seems adequate not to reject hypothesis 1.

Hypothesis 2. Surface soil water movements can be monitored and quantified through rectified video image (RVI) analysis based on models developed through CRS-GSM.

Creating accurate DEMs constitutes a first step to a better understanding of ecohydrological processes involving the upper soil (Kamphorst et al., 2005; Martin et al., 2008). The quality (precision, accuracy, resolution) needed for a DEM should be adequate for the purpose or application intended. Less precise smoothing techniques might be sufficient to achieve goals such as erosion-mediated soil loss (Warner, 1995; Rieke-Zapp and Nearing, 2005). In this study, the quality of terrain DEMs was evaluated in terms of its adequacy to support quantitative descriptions of water movements at the soil surface.

In the authors' experience, several of the GSM algorithms usually employed to generate smoothed DEMs, like polynomial fitting (Fan and Gijbels, 1995), inverse distance methods (Lam, 1983) and triangulation (Lawson, 1972) proved less accurate than kriging (Houlding,

2000). There is also a discrepancy among authors about how to measure the precision of a DEM representing the surface of a soil plot.

A test on the quality of a DEM obtained through a given method should ideally involve a comparative analysis with another DEM obtained by some other means assumed to be of higher accuracy and precision. CRS and laser scanning techniques were used by Aguilar et al. (2009); they found that both techniques yielded similar results and both performed worse on soils with high rugosity. They also found that DEMs generated through CRS were generally smoother than those obtained with laser scanning, an observation made earlier by Jester and Klik (2005) although they did not discuss the role of GSM techniques in smoothing quality. Both of those non-contact techniques seemed equally able to produce the required raw data for GSM of the soil surface, and both demanded similar experimental and sampling efforts (Brasington and Smart, 2003; Aguilar et al., 2009). In this study, z estimates accurate to under 0·1% and precise to less than 0·3% were obtained, based on a DEM obtained through CRS as compared to a true estimate obtained by an EVM procedure based on paired optical level estimates. A spatially distributed analysis of the DEM (Fig. 4(a)) did not show evidence of significant border or dome effects on the above-mentioned ranges of precision (Fig. 4(b) right). DEMs obtained through CRS in this study were adequate to estimate maps of water flow vectors. Fig. 5 shows visual agreement of these when overlaid on time-varying RVIs of water plumes generated by irrigation on experimental plots.

These results confirm that real-time video imagery (RVI) of runoff plumes of both laminar and rill flow generated during controlled irrigation experiments are adequate to study runoff dynamics; this is shown by Sidorchuk et al. (2008) who calculated hydrological parameters of water runoff streams and sediment transport in highly sloped samples of upper rendzina soils. They observed the movements of photographed floats on the runoff plumes and found them to be compatible with the basic theory about the hydrological processes involved, although they did not characterise the soil microtopography and its influence upon the results obtained. In this study, quantitative agreement (at a statistical significance of $p < 0{\cdot}01$) was also found between water flow orientation and water plume movements in field plots (Fig. 6).

Based on the above considerations, it does not seem appropriate to reject hypothesis 2. The application of equations (2) to (4) to water runoff, ponding and infiltration experiments and models in undisturbed field plots is the subject of continuing research at the National Patagonic Centre.

Conclusion

It is concluded that the CRS-GSM-RVI technique is a viable approach to estimate dynamic parameters of water runoff flow, ponding and infiltration in undisturbed field plots. Research applications to ecohydrology are anticipated (water redistribution among soil patches; soil micro-relief effects on water availability to plants; estimation of scaling factors to model soil surface hydrology; and material transport at the soil surface). The pertinence of using EVM statistics is indicated in assessing the precision and accuracy of DEMs obtained under field conditions through CRS and alternative techniques (optical scanner terrain surveying).

Acknowledgements

This project was funded by the National Council for Scientific and Technical Research (PIP 11420080100201) and by the National Agency for Promotion of Science and Technology (ANPCyT, Project PICT 1738-07) of Argentina.

REFERENCES

AGUILAR, M. A., AGUILAR, F. J. and NEGREIROS, J., 2009. Off-the-shelf laser scanning and close-range digital photogrammetry for measuring agricultural soils microrelief. *Biosystems Engineering*, 103(4): 504–517.

ARES, J., DEL VALLE, H. and BISIGATO, A., 2003. Detection of process-related changes in plant patterns at extended spatial scales during early dryland desertification. *Global Change Biology*, 9(11): 1643–1659.

ARIAS, P., ORDOÑEZ, C., LORENZO, H., HERRAEZ, J. and ARMESTO, J., 2007. Low-cost documentation of traditional agro-industrial buildings by close-range photogrammetry. *Building and Environment*, 42(4): 1817–1827.

BISIGATO, A., ARES, J. and BERTILLER, M., 2002. Assessment of pristine vegetation structure in semiarid shrublands based on spatial explicit modelling. *Phytocoenologia*, 32(4): 581–594.

BRASINGTON, J. and SMART, R. M., 2003. Close range digital photogrammetric analysis of experimental drainage basin evolution. *Earth Surface Processes and Landforms*, 28(3): 231–247.

CERDÁ, A. and GARCIA-FAYOS, P., 1997. The influence of slope angle on sediment, water and seed losses on badland landscapes. *Geomorphology*, 18(2): 77–90.

DEBLAUWE, V., BARBIER, N., COUTERON, P., LEJEUNE, O. and BOGAERT, J., 2008. The global biogeography of semi-arid periodic vegetation patterns. *Global Ecology and Biogeography*, 17(6): 715–723.

FAN, J. and GIJBELS, I., 1995. Data driven bandwidth selection in local polynomial fitting: variable bandwidth and spatial adaptation. *Journal of the Royal Statistical Society B*, 57(2): 371–394.

FEKRI, M. and RUIZ-GAZEN, A., 2006. Robust estimation in the simple errors-in-variables model. *Statistics & Probability Letters*, 76(16): 1741–1747.

FRERE, M. H., ROSS, J. D. and LANE, L. J., 1980. The nutrient submodel. Chapter 4 in *CREAMS: A Field Scale Model for Chemicals, Runoff, and Erosion from Agricultural Management Systems* (Ed. W. G. Knisel). USDA Conservation Research Report 26, Washington, DC. 640 pages: 65–87.

GBUREK, W. J. and SHARPLEY, A. N., 1998. Hydrologic controls on phosphorus loss from upland agricultural watersheds. *Journal of Environmental Quality*, 27(2): 267–277.

GOLLUSCIO, R. A., SALA, O. E. and LAUENROTH, W. K., 1998. Differential use of large summer rainfall events by shrubs and grasses: a manipulative experiment in the Patagonian steppe. *Oecologia*, 115(1–2): 17–25.

GOOVAERTS, P., 1997. *Geostatistics for Natural Resources Evaluation*. Oxford University Press, New York. 483 pages.

HANNAH, D. M., WOOD, P. J. and SADLER, J. P., 2004. Ecohydrology and hydroecology: a ''new paradigm''? *Hydrological Processes*, 18(17): 3439–3445.

HELMING, K., ROTH, C. H., WOLF, R. and DIESTEL, H., 1993. Characterization of rainfall–microrelief interactions with runoff using parameters derived from digital elevation models (DEMs). *Soil Technology*, 6(3): 273–286.

HENG, B. C. P., CHANDLER, J. H. and ARMSTRONG, A., 2010. Applying close range digital photogrammetry in soil erosion studies. *Photogrammetric Record*, 25(131): 240–265.

HOULDING, S. W., 2000. *Practical Geostatistics. Modelling and Spatial Analysis*. Springer, Berlin. 159 pages.

HUANG, C., WHITE, I., THWAITE, E. G. and BENDELI, A., 1988. A noncontact laser system for measuring soil surface topography. *Journal of Soil Science Society of America*, 52(2): 350–355.

ISAAKS, E. H. and SRIVASTAVA, R. M., 1989. *An Introduction to Applied Geostatistics*. Oxford University Press, New York. 561 pages.

JESTER, W. and KLIK, A., 2005. Soil surface roughness measurement—methods, applicability, and surface representation. *CATENA*, 64(2–3): 174–192.

KAMPHORST, E. C. and DUVAL, Y., 2001. Validation of a numerical method to quantify depression storage by direct measurements on moulded surfaces. *CATENA*, 43(1): 1–14.

KAMPHORST, E. C., CHADŒUF, J., JETTEN, V. and GUÉRIF, J., 2005. Generating 3D soil surfaces from 2D height measurements to determine depression storage. *CATENA*, 62(2–3): 189–205.

LAM, N. S.-N., 1983. Spatial interpolation methods: a review. *The American Cartographer*, 10(2): 129–149.

LAWSON, C. L., 1972. *Generation of a triangular grid with application to contour plotting*. Jet Propulsion Laboratory Internal Technical Memorandum No. 299, Pasadena, California. 914 pages.

LI, X.-Y., GONZÁLEZ, A. and SOLÉ-BENET, A., 2005. Laboratory methods for the estimation of infiltration rate of soil crusts in the Tabernas Desert badlands. *CATENA*, 60(3): 255–266.

LIU, Q. Q. and SINGH, V. P., 2004. Effect of microtopography, slope length and gradient, and vegetative cover on overland flow through simulation. *Journal of Hydrologic Engineering*, 9(5): 375–382.

MARES, M. A., MORELLO, J. and GOLDSTEIN, G., 1985. The Monte Desert and other subtropical semi-arid biomes of Argentina, with comments on their relation to North American arid areas. Chapter 6 in Hot Deserts and Arid Shrublands. Ecosystems of the World, Vol. 12A (Eds. M. Evenari, I. Noy-Meir & D. W. Goodall). Elsevier, Amsterdam, the Netherlands. 365 pages: 203–237.

MARTIN, Y., VALEO, C. and TAIT, M., 2008. Centimetre-scale digital representations of terrain and impacts on depression storage and runoff. *CATENA*, 75(2): 223–233.
MEREL, A. P. and FARRES, P. J., 1998. The monitoring of soil surface development using analytical photogrammetry. *Photogrammetric Record*, 16(92): 331–345.
PLANCHON, O., ESTEVES, M., SILVERA, N. and LAPETITE, J.-M., 2002. Microrelief induced by tillage: measurement and modelling of Surface Storage Capacity. *CATENA*, 46(2–3): 141–157.
PUIGDEFÁBREGAS, J., AGUILERA, C., BRENNER, A., CLARK, S. C., CUETO, M., DELGADO, L., DOMINGO, F., GUTIÉRREZ, L., INCOLL, I. D., LÁZARO, R., NICOLAU, J. M., SÁNCHEZ, G., SOLÉ, A. and VIDAL, S., 1996. The Rambla Honda field site: interactions of soil and vegetation along a catena in semi-arid SE Spain. Chapter 5 in *Mediterranean Desertification and Land Use* (Eds. C. J. Brandt & J. B. Thornes). Wiley, Chichester, UK. 572 pages: 137–168.
PUIGDEFÁBREGAS, J., DEL BARRIO, G., BOER, M. M., GUTIÉRREZ, L. and SOLÉ-BENET, A., 1998. Differential responses of hillslope and channel elements to rainfall events in a semi-arid area. *Geomorphology*, 23(2–4): 337–351.
REILLY, P. M., REILLY, H. V. and KEELER, S. E., 1993. Parameter estimation in the error-in-variables model. *Applied Statistics*, 42(4): 693–709.
RIEKE-ZAPP, D. H., WEGMANN, H., SANTEL, F. and NEARING, M. A., 2001. *Digital photogrammetry for measuring soil surface roughness*. Proceedings of the American Society of Photogrammetry & Remote Sensing 2001 Conference: Gateway to the New Millennium, St Louis, Missouri. 8 pages.
RIEKE-ZAPP, D. H. and NEARING, M. A., 2005. Digital close range photogrammetry for measurement of soil erosion. *Photogrammetric Record*, 20(109): 69–87.
RITSEMA, C. J. and DEKKER, L. W., 1995. Distribution flow: a general process in the top layer of water repellent soils. *Water Resources Research*, 31(5): 1187–1200.
SCHLESINGER, W. H., ABRAHAMS, A. D., PARSONS, A. J. and WAINWRIGHT, J., 1999. Nutrient losses in runoff from grassland and shrubland habitats in southern New Mexico: I. rainfall simulation experiments. *Biogeochemistry*, 45(1): 21–34.
SIDORCHUK, A., SCHMIDT, J. and COOPER, G., 2008. Variability of shallow overland flow velocity and soil aggregate transport observed with digital videography. *Hydrological Processes*, 22(20): 4035–4048.
SOLÉ-BENET, A., CALVO, A., CERDÁ, A., LÁZARO, R., PINI, R. and BARBERO, J., 1997. Influences of micro-relief patterns and plant cover on runoff related processes in badlands from Tabernas (SE Spain). *CATENA*, 31(1–2): 23–28.
STOJIC, M., CHANDLER, J. H., ASHMORE, P. and LUCE, J., 1998. The assessment of sediment transport rates by automated digital photogrammetry. *Photogrammetric Engineering & Remote Sensing*, 64(5): 387–395.
TONGWAY, D. J. and LUDWIG, J. A., 1999. Vegetation and soil patterning in semi-arid mulga lands in eastern Australia. *Australian Journal of Ecology*, 15(1): 23–34.
WACKROW, R. and CHANDLER, J. H., 2011. Minimising systematic error surfaces in digital elevation models using oblique convergent imagery. *Photogrammetric Record*, 26(133): 16–31.
WALLACH, R., GRIGORIN, G. and RIVLIN, J., 2001. A comprehensive mathematical model for transport of soil-dissolved chemicals by overland flow. *Journal of Hydrology*, 247(1–2): 85–99.
WARNER, W. S., 1995. Mapping a three-dimensional soil surface with handheld 35 mm photography. *Soil and Tillage Research*, 34(3): 187–197.
WEISBERG, S., 2005. *Applied Linear Regression*. Third edition. Wiley, Hoboken, New Jersey. 310 pages.
ZALEWSKI, M. and ROBARTS, R., 2003. Ecohydrology—a new paradigm for integrated water resources management. *Societas Internationalis Limnologia News*, 40(1): 1–5.
ZHAO, Y., PETH, S., HALLETT, P., WANG, X., GIESE, M., GAO, Y. and HORN, R., 2011. Factors controlling the spatial patterns of soil moisture in a grazed semi-arid steppe investigated by multivariate geostatistics. *Ecohydrology*, 4(1): 36–48.

Résumé

L'éco-hydrologie est une discipline émergente en sciences de l'environnement. Le micro-relief du sol joue un rôle dans plusieurs processus éco-hydrologiques comme la redistribution de l'eau de pluie, le déplacement des graines par les écoulements d'eau, l'érosion hydrique et la compétition des plantes pour l'eau. Les méthodes mécaniques et optiques pour caractériser la surface du sol et son influence sur ces processus sont consommatrices de temps et peuvent engendrer des modifications du relief du sol. Cette étude explore une méthodologie qui combine

des techniques sans contact de description de la micro-topographie (photogrammétrie rapprochée et modélisation géostatistique) avec l'analyse d'images vidéo, destinée à une description quantitative du mouvement et de l'infiltration des eaux de surface dans des parcelles de terrain non perturbées. La qualité numérique des résultats obtenus a été évaluée par les modèles de laboratoire représentant différentes formes élémentaires de terrain (bassin, colline, crête) ainsi que par des expériences d'infiltration et ruissellement dans des parcelles de terrain non perturbées. Des contraintes sont mises en évidence en ce qui concerne la détermination d'un ensemble minimal d'images numériques correctement orientées pour respecter les seuils de précision des cibles dans la modélisation de la micro-topographie du sol pour des applications éco-hydrologiques, de même que les conditions et l'organisation expérimentale appropriées pour l'obtention d'images vidéo des mouvements d'eau à la surface du sol. L'utilisation d'algorithmes géostatistiques pour l'analyse des processus éco-hydrologiques se produisant à la surface du sol est illustrée par les résultats obtenus sur des parcelles de terrain. La méthodologie présentée permet de caractériser et quantifier des processus écologiques où l'eau entre en jeu et se produisant à la surface, tout en évitant de perturber les sols. Elle a des applications potentielles en éco-hydrologie, en science de l'érosion et pour l'études des transports de matière dans l'environnement.

Zusammenfassung

Die Ökohydrologie ist eine junge Disziplin der Umweltwissenschaften. Das Mikrorelief eines Bodens ist für verschiedene Prozesse der Ökohydrologie bedeutend, wie z.B. der Umverteilung von Regenwasser, der Verteilung von Samen durch Wasserabfluss, der Wassererosion und dem Verdrängungswettbewerb von Pflanzen um Wasserressourcen. Mechanisch-optische Methoden zur Charakterisierung der Bodenoberfläche und ihres Einflusses auf die obigen Prozesse sind zeitaufwändig und können das Bodenrelief verändern. In diesem Forschungsbeitrag wird eine Methode der Kombination von kontaktfreien Techniken (Nahbereichsphotogrammetrie und geostatistische Modellierung) zur Beschreibung einer Mikro-Topographie beschrieben. Aus einer Videobildanalyse soll eine quantitative Analyse der Oberflächenwasserbewegung und der Infiltration in ungestörte Feldflächen durchgeführt werden. Die numerische Qualität der erzielten Ergebnisse wurde durch Labormodelle, die verschiedene elementare Landformen (Senke, Hügel und Kamm) repräsentieren und durch Infiltrationsexperimente in ungestörten Feldflächen getestet. Für diese ökohydrologischen Anwendungen werden die Anforderungen zur Bestimmung eines minimalen Satzes sorgfältig orientierter digitaler Bilder für die Modellierung der Mikro-Topographie wie auch die Bedingungen und experimentellen Anordnungen zur Erfassung geeigneter Videobilder zum Wasserabfluss an der Bodenoberfläche vorgestellt. Die Nutzung geostatischer Algorithmen zur Analyse der ökohydrologischen Prozesse wird an realen Beispielen vorgestellt. Die beschriebene Vorgehensweise erlaubt die Charakterisierung und Quantifizierung von ökohydrologischen Prozessen, unter Bewahrung der Oberflächenbeschaffenheit. Mögliche Anwendungen sind neben der Öko-Hydrologie, die Bodenerosionskunde und Studien zum Materialtransport.

Resumen

La eco-hidrología es una disciplina emergente en las ciencias ambientales. El microrrelieve del suelo es de interés para diversos procesos eco-hidrológicos como la distribución del agua de lluvia, desplazamientos de semillas a través del escurrimiento de agua, erosión hídrica y la competencia hídrica entre plantas. Los métodos ópticos-mecánicos para caracterizar la superficie topográfica del suelo y su incidencia en estos procesos requieren tiempo considerable y pueden alterar la superficie del suelo al ser aplicados. Este trabajo explora una metodología que combina técnicas sin contacto para describir la microtopografía (fotogrametría de objeto cercano, análisis de imágenes de videos y modelación geoestadística) con análisis de imágenes de video para formular análisis cuantitativos del movimiento superficial del agua e infiltración en parcelas no perturbadas en campo. La calidad numérica de los resultados obtenidos fue validada con modelos de laboratorio representando diversas geoformas (cuenca, cerro, cordón), así como con experimentos de infiltración-escorrentía en parcelas en campo. Se exponen los requisitos para definir un conjunto mínimo de imágenes digitales adecuadamente orientadas para alcanzar los umbrales de precisión necesarias en la modelación de la microtopografía del suelo, así como las condiciones y disposición experimental para obtener imágenes de vídeo del movimiento del agua sobre la superficie del suelo. Se ilustra el uso de algoritmos geoestadísticos para análisis de procesos eco-hidrológicos que ocurren en la superficie del suelo con resultados obtenidos de las parcelas en campo. La metodología presentada sirve para caracterizar y cuantificar procesos ecológicos relacionados con el agua que ocurren en la superficie del suelo, preservando sus condiciones inalteradas. Aplicaciones potenciales a eco-hidrología, ciencias de la erosión del suelo y estudios medioambientales de transporte de materiales.